Retraction

Retracted: Fault Diagnosis of Wind Turbine Gearbox Based on Multisensor Data Fusion

Journal of Control Science and Engineering

This article has been retracted by Hindawi following an investigation undertaken by the publisher [1]. This investigation has uncovered evidence of one or more of the following indicators of systematic manipulation of the publication process:

(1) Discrepancies in scope

(2) Discrepancies in the description of the research reported

(3) Discrepancies between the availability of data and the research described

(4) Inappropriate citations

(5) Incoherent, meaningless and/or irrelevant content included in the article

(6) Peer-review manipulation

The presence of these indicators undermines our confidence in the integrity of the article's content and we cannot, therefore, vouch for its reliability. Please note that this notice is intended solely to alert readers that the content of this article is unreliable. We have not investigated whether authors were aware of or involved in the systematic manipulation of the publication process.

Wiley and Hindawi regrets that the usual quality checks did not identify these issues before publication and have since put additional measures in place to safeguard research integrity.

We wish to credit our own Research Integrity and Research Publishing teams and anonymous and named external researchers and research integrity experts for contributing to this investigation.

The corresponding author, as the representative of all authors, has been given the opportunity to register their agreement or disagreement to this retraction. We have kept a record of any response received.

References

[1] R. Zhang and T. Zhou, "Fault Diagnosis of Wind Turbine Gearbox Based on Multisensor Data Fusion," *Journal of Control Science and Engineering*, vol. 2022, Article ID 5869958, 9 pages, 2022.

Research Article

Fault Diagnosis of Wind Turbine Gearbox Based on Multisensor Data Fusion

Ruimin Zhang [1] **and Tao Zhou** [2]

^{1}College of Mechanical and Electrical Engineering, Shihezi University, Shihezi 832003, Xinjiang, China
^{2}College of Information Science and Technology, Shihezi University, Shihezi 832003, Xinjiang, China

Correspondence should be addressed to Tao Zhou; 15085231210008@hainanu.edu.cn

In order to improve the operation efficiency of wind turbine gearbox and reduce the operation and maintenance cost of wind farm, a fault diagnosis system for wind turbine gearbox based on multisensor data fusion was proposed. First, the different time-domain statistical characteristic parameters of the original vibration signal were calculated, and the information fusion of the feature level and the data level was carried out by means of parallel superposition to obtain the fused data set. Second, a fault classification and recognition model based on GMO-KELM was established by using the fusion data set. Finally, the proposed method was used to monitor the status of the measured data of the gearbox on the vibration test bed of rotating machinery. The experimental results showed that the average training accuracy and the average test accuracy of GMO-KELM method were 100% and 95.58%, respectively, which were much higher than those of other methods. Through experiments and analyses, it was shown that the proposed method was effective and feasible. Compared with other similar methods, the proposed method had the best classification performance.

1. Introduction

Although the failure rate of wind turbine gearbox is relatively low, it can lead to the longest downtime and the highest maintenance costs. Therefore, an effective method is needed to monitor its operating status and send out early warning information before failure [1]. Vibration monitoring is an effective method to monitor the condition of wind turbine gearbox. However, most of gearboxes in early service of wind turbine is not equipped with a vibration monitoring system, so it is difficult to obtain the corresponding vibration signal. Based on supervisory control and data acquisition (SCADA), the fault warning method of the wind turbine gearbox in the SCADA system is still concerned. A common method is that multiple parameters of SCADA are integrated with a machine learning method to establish a model of a certain state variable during normal operation and state assessment and fault warning are conducted by monitoring the dynamic residual change between

the predicted value and actual value [2]. However, the method of integrating multiple monitoring parameters into a single predicted value of monitoring parameters is often difficult to characterize the operating state of the gearbox comprehensively and effectively. With the help of the powerful feature learning and deep mining capabilities of deep learning, it is an effective method to fuse multiple monitoring quantities into corresponding monitoring predicted values by deep learning method. It is an effective method to carry out wind turbine gearbox fault warning by analyzing the reconstruction error between model predicted values and actual values, as shown in Figure 1. Woo et al. constructed the network model of the gearbox with the limited depth Boltzmann machine, combined with the adaptive threshold analysis of the model reconstruction error, and gearbox fault detection was achieved [3]. Bajaj et al. realized early fault warning of gearbox by constructing the self-coding network model and combining the threshold analysis method based on an extremum theory. As the model
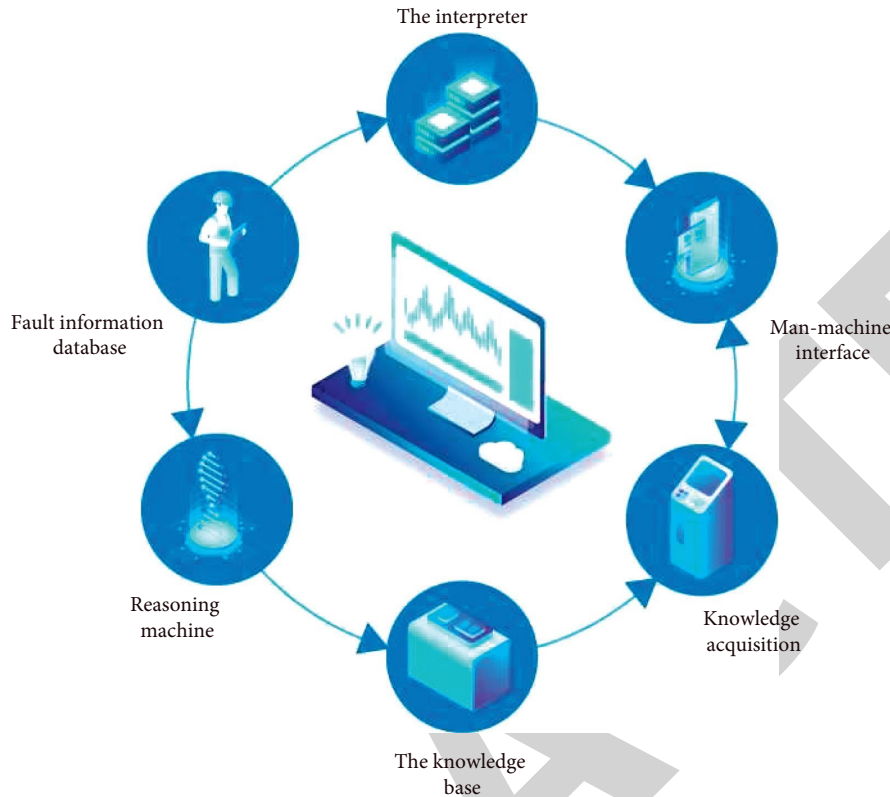
FIGURE 1: Fault diagnosis of the wind turbine gearbox.

fusion output is multiple monitoring quantities, the abovementioned method can better comprehensively represent the operating state of the gearbox [4]. However, the SCADA data of wind turbine gearbox in normal operation not only have stable data structure characteristics but also satisfy some data distribution rules. In the fusion process, the above deep learning model only focuses on the structural characteristics of the data and fails to fully mine the data distribution rules. As a result, the fusion model is too sensitive to the data set and has poor warning robustness when facing time-varying wind turbine gearbox monitoring data in practical applications. Variational autoencoder (VAE) networks can not only learn the structural features and internal correlation between data sets deeply but also make the network hidden layer variables learn the distribution rules of original data by adding constraints. Moreover, the model warning robustness is stronger [5]. Therefore, in the research, multiple SCADA monitoring quantities were fused into corresponding monitoring predicted values by a deep variational self-coding network. Reconstruction errors between model predicted values and actual values were analyzed and threshold evaluation criteria based on the Gauss distribution theory were combined to realize early fault warning of gearboxes.

2. Literature Review

Truong et al. made fault prediction based on the monitoring data collected by SCADA and divided the prediction results into three stages of progressively increasing fault levels for

warning based on multidata mining technology [6]. Nie et al. predicted potential failures of wind turbines by FFT, wavelet transform, and least mean square error technology on the basis of speed and wind speed signals and power collected by the intermediate frequency and SCADA (vibration, temperature, power, etc.) [7]. Liu and Corbita proposed an intelligent state monitoring technology based on EMD, by monitoring the output power and rotational speed of the wind turbine in real time, and combining the wavelet adaptive filtering technology to extract the fault features, the nonstationary and nonlinear signals of the wind turbine are accurately and effectively processed [8]. Chilamkurti et al. developed a complete, effective, and simple remote monitoring system for mechanical structure failure, temperature, smoke concentration, and environmental abnormality of the wind power gearbox by effectively combining and analyzing temperature signal, vibration signal, video monitoring of surrounding environment, and monitoring of surrounding smoke concentration [9]. Koukoura et al. analyzed common failure forms of fan spindle bearings from the perspective of time domain and frequency domain, providing a good idea for bearing fault diagnosis in terms of signal analysis [10]. Zhao et al. realized a simple fault diagnosis model like "black box call" through mixed programming of VC++ and MATLAB, which was not only easy to use but also improved a lot in accuracy [11]. Bradha et al. realized fault diagnosis of the gearbox by combining empirical mode decomposition (EMD) and the wavelet denoising method. First, the original vibration signal was denoised. Then, the denoising signal was decomposed by EMD and the envelope signal was

obtained by the Hilbert transform of the modal signal containing fault features. Finally, power spectrum analysis was carried out on the envelope signal. The results showed that the corresponding fault characteristic frequency could be found better [12].

In order to improve the fault diagnosis rate and solve the problem that the kernel parameters and penalty factors were too sensitive to KELM model, the GMO-KELM method was applied to the fault diagnosis of wind turbine gearbox based on the time-domain feature statistical analysis and multi-sensor information fusion technology. Compared with other similar methods, this method had the best classification performance.

3. Research Methods

3.1. Time-Domain Statistical Analysis and Multisensor Information Fusion Technology. When a wind turbine gearbox fails, the vibration energy will change greatly. The time-domain statistical index can reflect the change of vibration intensity. However, even for the same fault, different gearbox models will lead to inconsistent fault judgment criteria, which aggravates the difficulty of fault diagnosis [13]. Information fusion is a method to semiautomatically or automatically convert information at different time points and from different sources into a form by using decision level fusion, feature level fusion or data level fusion technology. More effective information can be obtained by optimizing the combination of information. In order to improve the accuracy of fault classification, the multisensor information fusion data set is obtained based on the time-domain statistical eigenvalues reflecting vibration intensity and combined with data level and feature-level fusion technology. The specific process is as follows.

(1) m different acceleration sensors are used to collect vibration acceleration signal vector $y(t)$ from different positions, as shown in formula.

$$\mathbf{y}(t) = \begin{bmatrix} y_1(t) & y_2(t) & \cdots & y_m(t) \end{bmatrix}. \tag{1}$$

(2) For the collected multisource finite discrete sequence signals, the original fault information matrix is shown in formula.

$$\mathbf{y}(t) = \begin{bmatrix} y_{1,1} & y_{1,2} & \cdots & y_{1,m} & c_1 \\ y_{2,1} & y_{2,2} & \cdots & y_{2,m} & c_2 \\ \vdots & \vdots & \vdots & \vdots \\ y_{M,1} & y_{M,2} & \cdots & y_{M,m} & c_M \end{bmatrix}. \tag{2}$$

In Formula (2), m is the total signal length collected by each sensor. c_i indicates different fault classification modes, $i = 1, 2, \ldots, M$.

(3) Thirteen important statistical characteristic values of vibration intensity are calculated, including root mean square value (y_{rms}), variance value (σ_2), peak index (C), pulse index (I), kurtosis index (y_q), mean value (y_i), maximum value (y_{max}), minimum value (y_{min}), peak-to-peak value (y_{pp}), root amplitude

(y_r), average amplitude (y^*), waveform index (K), and margin index (L), where N represents the calculated length of each index, as shown in formula.

$$y_{rms} = \left(\frac{1}{N} \sum_{i=1}^{N} y_i^2 \right)^{1/2}. \tag{3}$$

$$\sigma_2 = \frac{1}{N} \sum_{i=1}^{N} \left(y_i - \frac{1}{N} \sum_{i=1}^{N} y_i \right)^2. \tag{4}$$

$$\begin{cases} C = \dfrac{\max|y_i|}{y_{rms}} \\[2mm] I = \dfrac{\max|y_i|}{(1/N) \sum_{i=1}^{N} |y_i|} \end{cases} \tag{5}$$

$$\begin{cases} y_q = \dfrac{1}{N} \sum_{i=1}^{N} \dfrac{(y_i - \overline{y}_i)^4}{\left(1/N \sum_{i=1}^{N} y_i^2 \right)^2}, \\[4mm] \overline{y}_i = \dfrac{1}{N} \sum_{i=1}^{N} y_i. \end{cases} \tag{6}$$

$$\begin{cases} y_{max} = \max\{y_i\}, \\ y_{min} = \min\{y_i\}, \end{cases} \tag{7}$$

$$\begin{cases} y_{pp} = y_{max} - y_{min} \\[2mm] y_r = \left(\dfrac{1}{N} \sum_{i=1}^{N} |y_i|^{1/2} \right)^2 \end{cases} \tag{8}$$

$$\left\{ y_* = \frac{1}{N} \sum_{i=1}^{N} |y_i| K = \frac{y_{rms}}{y_*} I = \frac{\max|y_i|}{y_r}. \right. \tag{9}$$

(4) Based on the parallel superposition method and combining the feature level and data-level fusion technology, the multisensor information fusion data $\mathbf{R}_y$ is obtained, where $\mathbf{R}_{y,m}$ represents the information fusion generation of the m th sensor and R_m represents the time-domain feature index value calculated according to the data of the m th sensor.

$$\mathbf{R}_{y,m} = \begin{vmatrix} R_m(1,1) & R_m(1,2) & \cdots & R_m(1,13) & c_{1,m} \\ R_m(2,1) & R_m(2,2) & \cdots & R_m(2,13) & c_{2,m} \\ \vdots & \vdots & \vdots & \vdots \\ R_m(\varepsilon,1) & R_m(\varepsilon,2) & \cdots & R_m(\varepsilon,13) & c_{\varepsilon,m} \end{vmatrix},$$

$$\mathbf{y}(t) \leftrightarrow \mathbf{R}_y = \mathbf{R}_{y,1} \quad \mathbf{R}_{y,2} \quad \cdots \quad \mathbf{R}_{y,m} \quad c_t, m,$$

$$\varepsilon = \frac{M}{N} \mathbf{R}_y \in \mathbf{R}^{(M/N) \times (13m+1)}. \tag{10}$$

3.2. KELM Method and GMO-KELM Method

3.2.1. KELM Method. KELM is a single hidden layer feedforward neural network (SLFNs) learning algorithm, which is further put forward on the basis of ELM. The introduction of kernel function not only can reduce the computational complexity, but also increase the stability and robustness of the classification model. It has a better generalized performance. Therefore, in the research, the KELM method is adopted to conduct fault classification modeling for wind turbine gearbox [14, 15].

Any samples of different N can be expressed as (x_i, t_i), in which $x_i = [x_{i1}, x_{i2}, \ldots, x_{in}]^T \in \mathbf{R}^n$, $t_i = [t_{i1}, t_{i2}, \ldots, t_{im}]^T \in \mathbf{R}^m$. The weight vector between the ith hidden node and the input node is expressed as $w_i = [w_{i1}, w_{i2}, \ldots, w_{ik}]^T$. The weight vector between the i_{th} hidden node and the output node is expressed as $\beta_i = [\beta_{i1}, \beta_{i2}, \ldots, \beta_{im}]^T$. The neuron threshold of the *ith* hidden layer is represented as b_i. y_j represents the output of the network. n, k, and m represent the number of nodes in the input layer, hidden layer and output layer respectively. $g(x)$ represents the sigma activation function and H represents the output matrix of neurons in the hidden layer.

It can be seen from the above that the function of the basic ELM classification model is as follows (13), where $h(\cdot)$ represents the output function of the node of the hidden layer.

$$\mathbf{y}_j = \sum_{i=1}^{k} \boldsymbol{\beta}_i g_i(x_j) = \sum_{i=1}^{k} \boldsymbol{\beta}_i g(\mathbf{w}_i \mathbf{x}_j + b_i) = \sum_{i=1}^{k} \boldsymbol{\beta}_i h_i(\mathbf{x}) = h(\mathbf{x})\boldsymbol{\beta}_j,$$
$$j = 1, 2, \ldots, m. \tag{11}$$

Zero error mean value $\sum_{j=1}^{k} \mathbf{y}_j - \mathbf{t}_j = 0$ is used to ensure the accuracy of regression prediction. So, b_i, $\mathbf{w}_i$ and β_i are expressed as:

$$\sum^{k} \boldsymbol{\beta}_i g(\mathbf{w}_i \mathbf{x}_j + b_i) = \mathbf{t}_j, \quad j = 1, 2, \ldots, N. \tag{12}$$

$$H\beta = T. \tag{13}$$

In the formula below,

$$\mathbf{H}(w_1, w_2, \ldots, w_k, b_1, b_2, \ldots, b_k, x_1, x_2, \ldots, x_N)$$
$$= \begin{bmatrix} g(w_1 x_1 + b_1) & \cdots & g(w_k x_1 + b_k) \\ \vdots & & \vdots \\ g(w_1 x_N + b_1) & \cdots & g(w_k x_N + b_k) \end{bmatrix}_{N \times k} \tag{14}$$

$$\boldsymbol{\beta} = \begin{bmatrix} \boldsymbol{\beta}_1^T & \boldsymbol{\beta}_2^T & \cdots & \boldsymbol{\beta}_k^T \end{bmatrix}_{k \times m}^{T \times m}$$
$$\mathbf{T} = \begin{bmatrix} \mathbf{t}_1^T & \mathbf{t}_2^T & \cdots & \mathbf{t}_N^T \end{bmatrix}_{N \times m}^T. \tag{15}$$

The weight vector of the output layer is expressed as follows:

$$\boldsymbol{\beta} = \mathbf{H}^* \mathbf{T}. \tag{16}$$

In the formula, $\mathbf{H}^*$ is the generalized inverse, which is expressed as follows:

$$\mathbf{H}^* = \mathbf{H}^T \left(\frac{\mathbf{I}}{C} + \mathbf{H}\mathbf{H}^T \right)^{-1}. \tag{17}$$

In the formula, C is the cost parameter related to stable performance and generalized performance and I is the diagonal matrix.

In ELM, matrix H is generated through the random assignment. The uncertainty of assignment will lead to different matrices H each time produced by ELM technology for modeling, resulting in different weight vectors β of output layer. It leads to unsatisfactory generalization ability and stable performance of the ELM model [16]. In order to improve the state, matrix H in the ELM model is replaced by kernel matrix ELM Ω_{ELM} and input samples are mapped to a high-dimensional kernel space by kernel function. The kernel matrix of the KELM method and its elements Ω_{ij}, neural network characteristic Formula $y(x)$ and basic kernel function $K(x_i, x_j)$ are, respectively, expressed as follows, where γ is the kernel parameter and $K(x_i, x_j)$ is the radial basis function.

$$\begin{cases} \Omega_{\mathrm{ELM}} = \mathbf{H}^T, \\ \Omega_{ij} = h(x_i)h(x_j) = K(x_i, x_j), \end{cases} \tag{18}$$

$$y(x) = h(x)\mathbf{H}^T \left(\frac{\mathbf{I}}{C} + \mathbf{H}\mathbf{H}^T \right)^{-1} \mathbf{T},$$
$$= \begin{bmatrix} K(x, x_1) \\ K(x, x_2) \\ \vdots \\ K(x, x_N) \end{bmatrix} \left(\frac{\mathbf{I}}{C} + \Omega_{\mathrm{ELM}} \right)^{-1} \mathbf{T}, \tag{19}$$

$$K(x_i, x_j) = \exp\left(-\frac{\|x_i - x_j\|^2}{2\gamma^2} \right). \tag{20}$$

3.2.2. GWO-KELM Method. Although the existence of the kernel function will enhance the stability of the model structure, it will also cause the implementation of the KELM method to be very sensitive to parameter setting [17]. In order to avoid the fluctuation of network structure caused by a random assignment, GWO is used to optimize the γ and C parameters of KELM to further improve the robustness and stability of KELM model.

GWO is a new metaheuristic method proposed by Mirjalili et al. It simulates the social hierarchy and hunting mechanism of gray wolves in nature, mainly including wandering behavior, calling behavior, and siege behavior. A typical gray wolf social dominant hierarchy consists of Alpha, Beta, Delta, and Omega layers, which represents the best solution, the second and third best solution and the remaining candidate solutions, respectively [18]. In order to simulate the siege behavior of gray wolves, the following formula is proposed.
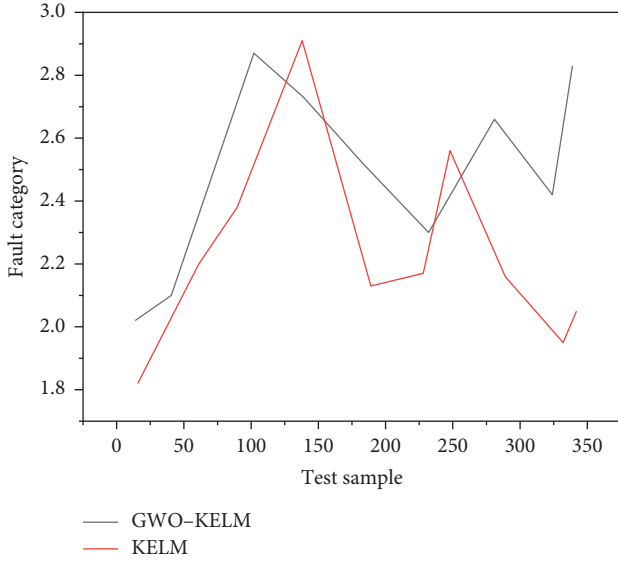
Figure 2: Diagnosis rate of the GWI-KELM method and diagnosis rate of the KELM method.

$$\begin{cases} \mathbf{D} = \left|2\,\mathrm{rand}\,(0,1)\mathbf{X}_{\mathrm{prey}}\,(t) - \mathbf{X}_{\mathrm{wolf}}\,(t)\right|, \\ \mathbf{X}_{\mathrm{wolf}}\,(t+1) = \mathbf{X}_{\mathrm{prey}}\,(t) - 2\mathbf{a}\,(\mathbf{ran}\,\mathbf{d}\,(0,1) - \mathbf{a})\mathbf{D}. \end{cases} \tag{21}$$

In Formula (23), D is the distance between wolf and prey. t is the number of iterations. Rand $(0, 1)$ represents a randomly generated vector between $[0, 1]$. $\mathbf{X}_{\mathrm{prey}}$ is the position vector of prey. $\mathbf{X}_{\mathrm{wolf}}$ is the position vector of gray wolf. a represents a linear decrement from 2 to 0 during each iteration.

Assuming that the wolf pack $\mathbf{X}_{\mathrm{wolf}} = [\mathbf{X}_1, \mathbf{X}_2, \ldots, \mathbf{X}_l]$ consists of l gray wolves, when the position of the gray wolf $\mathbf{X}_i$ is updated, the distance between the gray wolf X_i and the three wolves, $\mathbf{X}_{\mathrm{alpha}}$, $\mathbf{X}_{\mathrm{beta}}$, and $\mathbf{X}_{\mathrm{delta}}$ is first calculated as shown in equations (24) to (26). After calculating the distance, the position of X_1 needs to be updated as shown in equations (27) to (29).

$$\mathbf{D}_{\mathrm{alpha}} = \left|2\,\mathrm{rand}\,(0,1)\mathbf{X}_{\mathrm{alpha}} - \mathbf{X}\right|. \tag{22}$$

$$\mathbf{D}_{\mathrm{beta}} = \left|2\,\mathrm{rand}\,(0,1)\mathbf{X}_{\mathrm{beta}} - \mathbf{X}\right|. \tag{23}$$

$$\mathbf{D}_{\mathrm{delta}} = \left|2\,\mathrm{rand}\,(0,1)\mathbf{X}_{\mathrm{delta}} - \mathbf{X}\right|. \tag{24}$$

$$\mathbf{X}_{1,*} = \mathbf{X}_{\mathrm{alpha}} - 2\mathbf{a}\,(\mathbf{ran}\,\mathbf{d}\,(0,1) - \mathbf{a})\mathbf{D}_{\mathrm{alpha}}. \tag{25}$$

$$\mathbf{X}_{2,*} = \mathbf{X}_{\mathrm{beta}} - 2a\,(\mathbf{ran}\,\mathbf{d}\,(0,1) - \mathbf{a})\mathbf{D}_{\mathrm{beta}}. \tag{26}$$

$$\mathbf{X}_{3,*} = \mathbf{X}_{\mathrm{delta}} - 2\mathbf{a}\,(\mathbf{ran}\,\mathbf{d}\,(0,1) - \mathbf{a})\mathbf{D}_{\mathrm{delta}}. \tag{27}$$

$$\mathbf{X}(t+1) = \frac{\mathbf{X}_{1,*} + \mathbf{X}_{2,*} + \mathbf{X}_{3,*}}{3}. \tag{28}$$

In the abovementioned formulas, $\mathbf{X}_{1,*}$, $\mathbf{X}_{2,*}$, and $\mathbf{X}_{3,*}$, respectively, represents the vectors of the movement of the gray wolf $\mathbf{X}_{\mathrm{wolf}}$ to $\mathbf{X}_{\mathrm{alpha}}$, $\mathbf{X}_{\mathrm{beta}}$, and $\mathbf{X}_{\mathrm{delta}}$. X represents the position represented by the current solution [19].

Under the condition that the classification accuracy is optimal and the KELM wind turbine gearbox classification model is affected by the choice of parameter combination γ and C, GWO is adopted in the research to optimize the optimal parameter combination of the KELM classification model. The fitness function is selected as follows.

$$\begin{cases} \max \quad s(C, \gamma) = \dfrac{C_{\mathrm{r}}}{T_{\mathrm{t}}} \times 100\% \\ \\ \text{s.t.} \quad \begin{aligned} &C \in [C_{\min}, C_{\max}] \\ &\gamma \in [\gamma_{\min}, \gamma_{\max}]. \end{aligned} \end{cases} \tag{29}$$

In Formula (13), $[C_{\min}, C_{\max}]$ and $[\gamma_{\min}, \gamma_{\max}]$ are, respectively, the value range of cost parameter C and core parameter γ. C_r is the number of correctly classified samples. T_t is the number of all samples.

The program is run in the MATLAB R2017a environment, as shown in Figure 2. The diagnosis results show that GWOKELM method has a better predictive performance.

3.3. Wind Turbine Gearbox Fault Diagnosis Model Based on GMO-KELM.
The cost parameter C and the kernel parameter γ in the KELM fault diagnosis model are arbitrarily given and the setting of the initial parameter has a direct impact on the structure of KELM model [20]. In order to select the optimal parameters, the KELM optimization method based on GWO is adopted and its process is shown in Figure 3.

The specific steps of diagnosis are as follows.

(1) Vibration signal collection

According to the rotational speed of different parts of the rotating mechanism, different types of acceleration sensors are selected to collect vibration acceleration signals of the gearbox and define the fault classification.

(2) Multisensor data information fusion Formula (3) to formula (9) are used to calculate the statistical characteristic values reflecting vibration intensity. Moreover, the fusion of feature level and data level is carried out by parallel superposition to obtain the gearbox vibration fusion data set [21].

(3) Normalization processing The data set of information fusion is normalized to obtain preprocessed data samples for testing and training of the fault diagnosis model.

(4) The topological structure of KELM is determined. By using formula (13), KELM parameters γ and C are optimized by GWO, and the optimal parameters are obtained. The root-mean-square error is used as the standard to judge the fault classification accuracy.

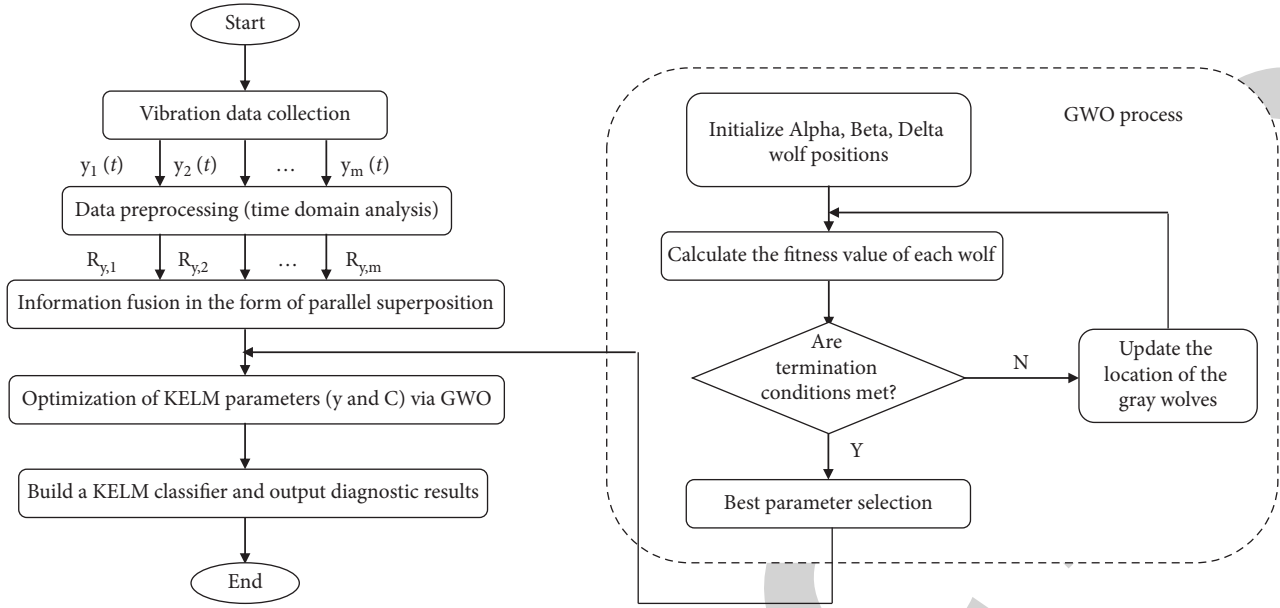(5) Training data sets and test data sets are set up in proportion. KELM fault diagnosis model is

FIGURE 3: Flow of the improved GMO-KELM method.

TABLE 1: Description of gearbox faults.

Failure category	Fault components	Failure mode	Input speed/(r·min^{-1})	Load/kW
1	Big gear Z_1 Pinion gear Z_2	Pitting of big gear Pinion wear	1 470,880,825	0,0,0.103
2	Big gear Z_1	Pitting of big gear	1 500,880,834	Small gear Z_2
3	Big gear Z_1	Big gear is broken	1 470,878,840	0,0,0.103
4	Pinion gear Z_2	Pinion wear	1 478,881,830	0,0,0.103
5	Normal	Normal	1 475,880,800	0,0,0.103
6	Big gear Z_1 Pinion gear Z_2	Big gear is broken Pinion wear	1 474,878,812	0,0,0.103

established. Moreover, fault diagnosis classification of gear boxes is carried out using this model.

3.4. Example Verification.
A variety of rotating machinery states and vibration can be rapidly simulated. Moreover, the health status and failure type of the equipment can be determined by analyzing the collected data signals [22]. In the research, the vibration acceleration signal of the gearbox is collected by the rotating machinery vibration test-bed device and the sampling frequency is set as 5.12 kHz. The fault pattern recognition of the gearbox is carried out based on the GWI-KELM method. Moreover, compared with many other similar methods, the example shows that the method has the best classification performance.

3.4.1. Experimental Device Platform.
The rotating machinery vibration test equipment platform is composed of the gear box, variable speed drive motor, magnetic powder torque device, and rotating shaft, etc. The platform can simulate a variety of failure modes of the gear box and can manually adjust the load torque.

The configuration of the gearbox is as follows. The number of teeth of the input gear (Z1) is 55, the number of teeth of the output gear (Z2) is 75, and the modulus is 2. Oil immersion lubrication is adopted. In the experiment, an AC

frequency conversion motor with a power of 0.75 KW drives the gear box to rotate. 5, 379, 072 gear vibration acceleration signals were obtained by five acceleration sensors installed on the motor side bearing of the input shaft, the motor side bearing of the output shaft, the load side bearing of the input shaft, the Y side of the load bearing of the output shaft and the X side of the load bearing of the output shaft respectively [23].

3.4.2. Data Acquisition and Preprocessing.
Through the abovementioned experimental device, the complex working conditions of the gearbox are fully taken into account and 6 different fault types are simulated under the conditions of variable load and speed, as shown in Table 1, including complex faults that are difficult to diagnose [24]. According to formula (3) to formula (9), the characteristic parameters of different time-domain indicators are calculated with 512 behavior units of measurement. Moreover, the information of multiple sensors is fused by means of parallel superposition and a signal fusion matrix of 1751×66 is obtained. Using the fusion signal matrix, the KELM model is trained and tested.

4. Result Analysis

Based on the signal fusion matrix and randomly selected training samples, 80% of the data sets were taken as training
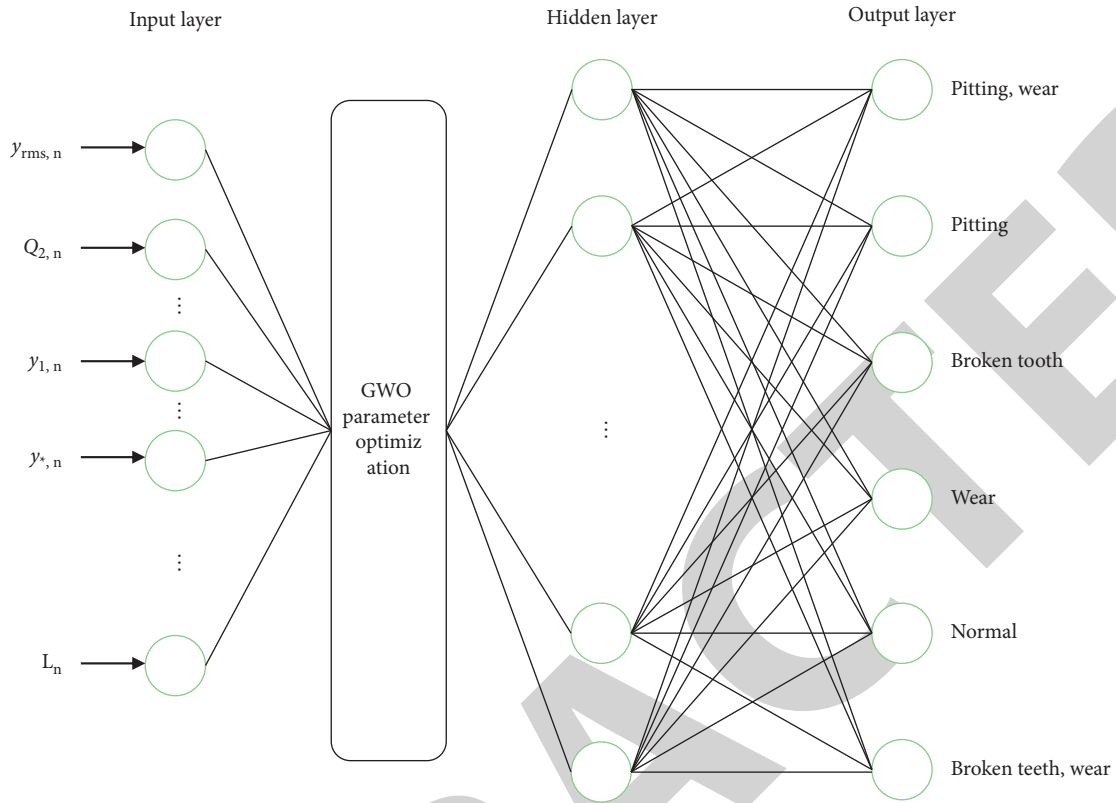
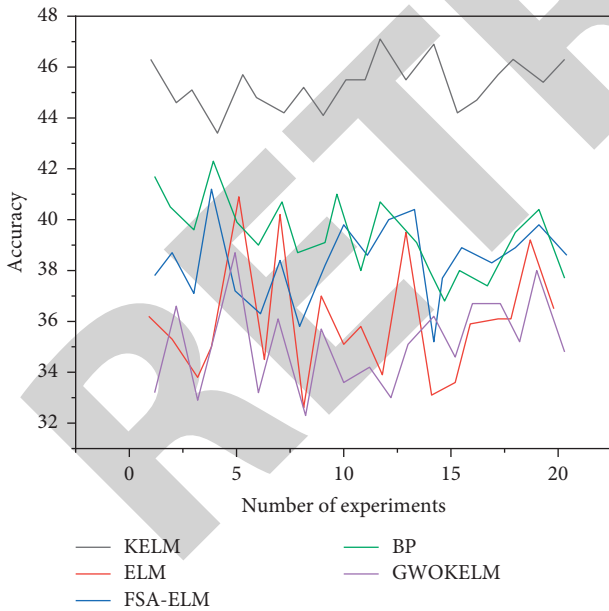Figure 4: Fault diagnosis model of GMO-KELM based on SLFNs.

Figure 5: The results of fault diagnosis.

samples and 20% of the data sets were taken as test samples. The fault diagnosis model of the GWA-KELM method was established. Moreover, the gearbox fault diagnosis models of KELM, ELM, the optimized ELM by fish swarm algorithm (FSA), and back propagation (BP) of the neural network were established. The experiments were repeated

20 times to verify the classification performance of various methods [25].

Parameters of the GWO method are set as follows. The maximum number of iterations is 50, the population size is 10, and the value range of parameter C is [0, 0.1] and [10, 1000], respectively. Root-mean-square error is taken as the judgment standard and equation (29) is used as fitness function to determine the optimal population value. Parameters of the KELM method are set as follows. Radial basis function (RBF) is selected as KELM kernel function, 65 time-domain characteristic indexes are taken as input, and 6 fault types are taken as output to construct the GMO-KELM fault diagnosis model, as shown in Figure 4. n indicates a sensor. In order to compare with the original vibration signal fault identification accuracy, the abovementioned methods are set as the same parameters and random vibration signal data dimension is 1751 ∗ 6 sets with five sensors of the original vibration signal as the input and six types of failure mode as the output. Each experiment is repeated 20 times. The diagnosis result is shown in Figure 5.

It can be seen from Figure 5 that KELM, ELM, ELM optimized by FSA, and BP neural network fault diagnosis models based on data fusion technology can be used for the gearbox fault diagnosis. The average training accuracy, average test accuracy, and average diagnosis time obtained by the five models can be seen as follows. (1) Based on the fusion data, the average training accuracy and test accuracy of GWOKELM method are 100% and 95.58%, respectively, which are much higher than other methods. (2) The

diagnosis accuracy based on the GWOKELM method is also higher than other methods for the gearbox state prediction based on raw data. (3) Compared with the FSA-ELM method, the method requires a slightly shorter diagnosis time. Compared with other similar methods, the method requires about the time of 100 s or so, but compared with the diagnosis accuracy, this effect is very small. Therefore, the method based on the combination of information fusion, time-domain analysis and GWOKELM can better reflect the fault situation and has the best classification performance.

5. Conclusions

Based on the multisensor data fusion technology and time-domain statistical analysis, combined with the GWI-KELM method, the fault diagnosis classification mode of wind turbine gearbox was effectively judged. On the premise of considering the complex and changeable working environment of wind turbine gearbox, the same fault and compound fault categories under different working conditions were investigated. The model was trained on the basis of the original data and fusion data from the gearbox measured on the rotating machinery vibration test bench. Compared with many other similar methods, the example showed that the proposed method had the best classification performance. The main work of the research was to verify the validity and practicability of the fault diagnosis method based on GWI-KELM and multisensor information fusion by using the gearbox vibration data on the test bench through MATLAB R2017a software. Moreover, the challenge of how to improve the efficiency of vibration monitoring of the unit and carry out the on-site verification of the method is the next research focus.

Data Availability

The data used to support the findings of this study are available from the corresponding author upon request.

Conflicts of Interest

The authors declare that they have no conflicts of interest.

References

[1] S. Baek, "System integration for predictive process adjustment and cloud computing based real time condition monitoring of vibration sensor signals in automated storage and retrieval systems," *International Journal of Advanced Manufacturing Technology*, vol. 113, no. 3, pp. 955–966, 2021.

[2] J. Zhao, D. Wang, F. Zhang et al., "Real-time and online lubricating oil condition monitoring enabled by triboelectric nanogenerator," *ACS Nano*, vol. 15, no. 7, pp. 11869–11879, 2021.

[3] A. Ji, W. L. Woo, E. W. L. Wong, and Y. T. Quek, "Rail track condition monitoring: a review on deep learning approaches," *Intelligence and Robotics*, vol. 1, no. 2, pp. 151–175, 2021.

[4] N. S. Bajaj, A. D. Patange, R. Jegadeeshwaran, K. A. Kulkarni, R. S. Ghatpande, and A. M. Kapadnis, "A bayesian optimized discriminant analysis model for condition monitoring of face milling cutter using vibration datasets," *Journal of Nondestructive Evaluation Diagnostics and Prognostics of Engineering Systems*, vol. 5, no. 2, pp. 1–12, 2021.

[5] C. Chellaswamy, T. S. Geetha, M. Surya Bhupal Rao, and A. Vanathi, "Optimized railway track condition monitoring and derailment prevention system supported by cloud technology," *Transportation Research Record*, vol. 2675, no. 4, pp. 346–361, 2021.

[6] H. Van Truong, N. Chi Hieu, P. Ngoc Giao, and N. Xuan Phong, "Unsupervised detection of anomalous sound for machine condition monitoring using fully connected u-net," *Journal of ICT Research and Applications*, vol. 15, no. 1, pp. 41–55, 2021.

[7] Z. Nie, Z. Shen, J. Li et al., "Using a single sensor for bridge condition monitoring via moving embedded principal component analysis," *Structural Health Monitoring*, vol. 20, no. 6, pp. 3123–3149, 2021.

[8] J. H. Liu and N. T. Corbita, "Performance analysis of different predictive models for condition monitoring of direct drive wind turbine generator," *Measurement and Control*, vol. 54, no. 3-4, pp. 374–384, 2021.

[9] A. Sharma, G. Rathee, R. Kumar et al., "A secure, energy and sla efficient (sese) e-healthcare framework for quickest data transmission using cyber-physical system," *Sensors*, vol. 19, no. 9, Article ID 2119, 2019.

[10] S. Koukoura, J. Carroll, A. Mcdonald, and S. Weiss, "Comparison of wind turbine gearbox vibration analysis algorithms based on feature extraction and classification," *IET Renewable Power Generation*, vol. 13, no. 14, pp. 2549–2557, 2019.

[11] L. Zhao, J. Gong, and H. Chong, "The extraction method of gearbox compound fault features based on eemd and cloud model," *Mathematical Problems in Engineering*, vol. 2020, no. 10, pp. 1–8, Article ID 6661975, 2020.

[12] M. Bradha, N. Balakrishnan, S. Suvi et al., "Experimental, computational analysis of butein and lanceoletin for natural dye-sensitized solar cells and stabilizing efficiency by IoT," *Environment, Development and Sustainability*, vol. 24, pp. 8807–8822, 2021.

[13] I. Singh, R. Jindal, K. Pandey, K. Agrawal, and K. Kukreja, "Revised grey wolf optimized svm-knn ensemble based automated diagnosis of breast cancer," *Ingénierie des Systèmes d'Information*, vol. 25, no. 2, pp. 275–284, 2020.

[14] J. Chen, J. Liu, X. Liu, X. Xu, and F. Zhong, "Decomposition of toluene with a combined plasma photolysis (CPP) reactor: influence of UV irradiation and byproduct analysis," *Plasma Chemistry and Plasma Processing*, vol. 41, no. 1, pp. 409–420, 2021.

[15] J. Yang, J. Wen, Y. Wang, B. Jiang, H. Wang, and H. Song, "Fog-based marine environmental information monitoring toward ocean of things," *IEEE Internet of Things Journal*, vol. 7, no. 5, pp. 4238–4247, 2020.

[16] J. Sansana, R. Rendall, Z. Wang, L. H. Chiang, and M. S. Reis, "Sensor fusion with irregular sampling and varying measurement delays," *Industrial and Engineering Chemistry Research*, vol. 59, no. 6, pp. 2328–2340, 2020.

[17] D. Zhao, "Rapid multimodal image registration based on the local edge histogram," *Mathematical Problems in Engineering*, vol. 2021, no. 9, pp. 1–9, Article ID 5598177, 2021.

[18] R. Huang, P. Yan, and X. Yang, "Knowledge map visualization of technology hotspots and development trends in China's textile manufacturing industry," *IET Collaborative Intelligent Manufacturing*, vol. 3, no. 3, pp. 243–251, 2021.

[19] L. Su, M. Li, S. Zhao, and T. Xie, "Distributed sensor local linear fusion detection of weak pulse signal in chaotic

background," *Journal of Sensors*, vol. 2021, no. 1, pp. 1–11, 2021.

[20] C. Shuai, Y. Yang, W. Zheng, and G. Fan, "Low altitude protection technology of anti-uavs based on multisource detection information fusion," *International Journal of Advanced Robotic Systems*, vol. 17, no. 5, pp. 139–149, 2020.

[21] W. Li, R. Zhang, and H. Lei, "Navigation switching strategy-based sins/gps/ads/dvl fault-tolerant integrated navigation system," *Journal of Sensors*, vol. 2021, no. 5, pp. 1–8, 2021.

[22] J. Jiao, J. Yue, D. Pei, and Z. Hu, "Application of feature fusion using coaxial vibration signal for diagnosis of rolling element bearings," *Shock and Vibration*, vol. 2020, pp. 1–14, Article ID 8831723, 2020.

[23] P. Hou, H. Ma, B. Liu, X. Chen, C. Zhu, and F. Tan, "Mechanical fault diagnosis of reactor core winding looseness based on multi-feature fusion and improved KELM," in *Proceedings of the IEEE Sustainable Power and Energy Conference (iSPEC)*Nanjing, China, 2021.

[24] X. Zhang, K. P. Rane, I. Kakaravada, and M. Shabaz, "Research on vibration monitoring and fault diagnosis of rotating machinery based on internet of things technology," *Nonlinear Engineering*, vol. 10, no. 1, pp. 245–254, 2021.

[25] M. Kowalski, B. Willett, B. Milgrom, and R. Ben-Dov, "Statistically efficient multisensor rotational bias estimation for passive sensors without target state estimation," *Journal of Advances in Information Fusion*, vol. 15, no. 2, pp. 73–90, 2021.